Micelle-to-Vesicle Transition Induced by Organic Additives in Catanionic Surfactant Systems

Haiqing Yin,[a] Sheng Lei,[a] Shengbao Zhu,[a] Jianbin Huang,*[a] and Jianpin Ye[b]

Abstract: A micelle-to-vesicle transition (MVT) induced by the addition of a series of apolar hydrocarbons (*n*-butylbenzene, *n*-hexane, *n*-octane, and *n*-dodecane) to the catanionic surfactant system *n*-dodecyltriethylammonium bromide/sodium *n*-dodecylsulfate (DTEAB/SDS) has been investigated for the first time by means of rheology and turbidity measurements, dynamic light scattering (DLS), and transmission electron microscopy (TEM). Interestingly, a MVT can take place within certain micellar regions, which are dependent on the structure and chain length of the hydrocarbon. However, these hydrocarbons are unable to induce a MVT in another catanionic surfactant system, namely, *n*-dodecyltriethylammonium bromide/sodium *n*-dodecylsulfonate (DTEAB/SDSO$_3$), in which the molecular interactions are weaker than in the DTEAB/SDS system. On the other hand, polar additives, such as *n*-octanol and *n*-octylamine, exhibit much higher efficiency and activity in inducing MVT than hydrocarbons in both DETAB/SDS and DTEAB/SDSO$_3$. Moreover, DLS, TEM, and time-resolved fluorescence quenching (TRFQ) results demonstrate that the ratio of vesicles to micelles in the system can be actively controlled by addition of polar additives. Possible mechanisms for the above phenomena are presented, and the potential application of controllable micelle/vesicle systems in the synthesis of tailored bimodal mesoporous materials is discussed.

Keywords: micelles · surfactants · vesicles

Introduction

Aqueous mixtures of anionic and cationic surfactants (referred to as catanionic surfactants) exhibit interesting phase behavior and properties, which mainly arise from the electrostatic interactions between the oppositely charged head groups. By adjusting the composition, these interactions can be tuned to produce various microstructures with characteristic geometries ranging from spherical to cylindrical to planar, which have been studied experimentally and theoretically[1] for their potential applications in many fields.

The nature of the transition between micelle and vesicle is of great importance in a number of practical applications[2] and of fundamental interest as well.[3] For catanionic surfactant systems, much attention has focused on the influence on the micelle-to-vesicle transition (MVT) or the vesicle-to-micelle transition (VMT) of changes in surfactant composition,[1a–e] temperature variation,[4] and salt addition.[5] However, in contrast to the many studies on organized transitions induced by the solubilization of organic additives in single-surfactant systems, little work[6] has been done on the influence of organic additives in catanionic surfactant systems, since organic additives, especially apolar hydrocarbons, are usually thought to have less effect in tailoring organized assemblies of catanionic surfactant systems due to the strong electrostatic attraction in this kind of systems.

Recently, we found[8] that the addition of some short-chain alcohols, such as 2-propanol, to some catanionic surfactant systems with precipitation not only influenced the phase behavior, but also transformed the precipitate into vesicles, which indicates that suitable additives may also play an important role in the transformation of organized assemblies in catanionic surfactant systems, in which strong electrostatic interactions exist. We have now systemically studied the effects of a series of hydrocarbons (*n*-butylbenzene, *n*-hexane, *n*-octane, and *n*-dodecane) and polar organic additives, such as *n*-octanol and *n*-octylamine, on the tran-

[a] H. Yin, S. Lei, S. Zhu, Prof. Dr. J. Huang
State Key Laboratory for Structural Chemistry of Unstable and Stable Species
College of Chemistry and Molecular Engineering
Peking University, Beijing 100871 (P. R. China)
Fax: (+86) 10-6275-1708
E-mail: JBHuang@pku.edu.cn

[b] J. Ye
Key laboratory of Photochemistry
Chinese Academy of Sciences, Beijing 100871 (P. R. China)

sition from micelle to vesicle in the catanionic surfactant systems *n*-dodecyltriethylammonium bromide/sodium *n*-dodecylsulfate (DTEAB/SDS) and *n*-dodecyltriethylammonium bromide/sodium *n*-dodecylsulfonate (DTEAB/SDSO₃). For the first time, it was found that apolar hydrocarbons can induce a MVT in the DTEAB/SDS system within certain ranges of surfactant composition, while they are unable to induce a MVT in the DTEAB/SDSO₃ system. Moreover, the polar organic additives are much more efficient in inducing a MVT than the hydrocarbons in both systems and can actively adjust the ratio of vesicles to micelles. Possible mechanisms for the above transitions are presented, based on the theory of the aggregate packing parameter, and the different effects of the additives on a MVT are explained. Furthermore, potential application of controllable micelle/vesicle systems in the synthesis of tailored bimodal mesoporous materials is discussed.

Results

Microstructures of the DTEAB/SDS system: The microstructures of the DTEAB/SDS system at a fixed total surfactant concentration C_{total} of 10 mmol were determined from the results (not shown) of turbidity measurements, dynamic light scattering (DLS), and transmission electron microscopy (TEM). A partial phase diagram for the variation of X_{DTEAB} ($X_{DTEAB} = C_{DTEAB}/C_{total}$) is shown in Figure 1. The vertical axis is the corresponding turbidity at 500 nm of each investigated sample. In Figure 1, transitions from micelle to vesicle and finally to precipitate can be observed as X_{DTEAB} approaches 0.5, which can be understood as the result of the neutralization of oppositely charged head groups. The micellar regions are at the two edges of the diagram with X_{DTEAB} ranges from 0 to 0.33 and from 0.85 to 1. The solubilization
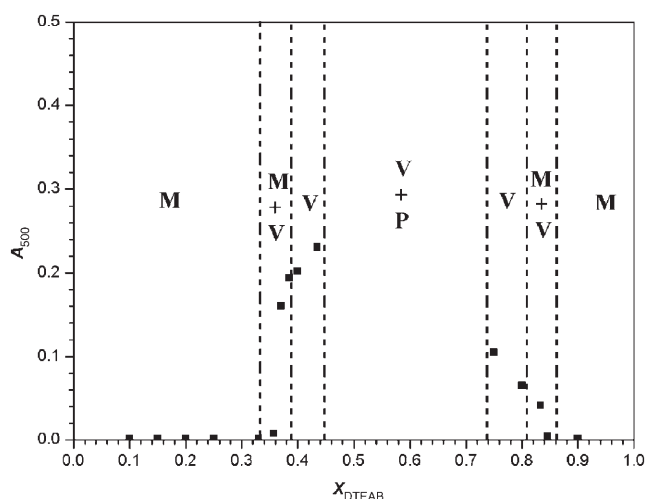
behaviors of various organic additives were studied in these regions.

MVT induced by addition of *n*-butylbenzene: The micellar DTEAB/SDS system with $C_{total} = 10$ mmol and $X_{DTEAB} = 0.25$ was selected for our study. Before addition of *n*-butylbenzene, the sample showed obvious non-Newtonian behavior in the steady-state rheological curve (Figure 2a): shear thickening at lower shear rates and shear-thinning at higher shear rates. This behavior is a typical property of rodlike micelles in dilute solutions and has been well investigated in other work.[9] On addition of *n*-butylbenzene to the mixed system, the non-Newtonian behavior becomes progressively weaker, and this suggests that the shape of aggregates becomes more symmetrical. In addition, a notable increase in absorbance at 500 nm on the addition of *n*-butylbenzene

Figure 1. Partial phase diagram of DTEAB/SDS with $C_{total} = 10$ mmol and varying X_{DTEAB}. ($X_{DTEAB} = C_{DTEAB}/C_{total}$; A_{500} is the turbidity at 500 nm of each investigated sample). M = micelle, V = vesicle, P = precipitate.
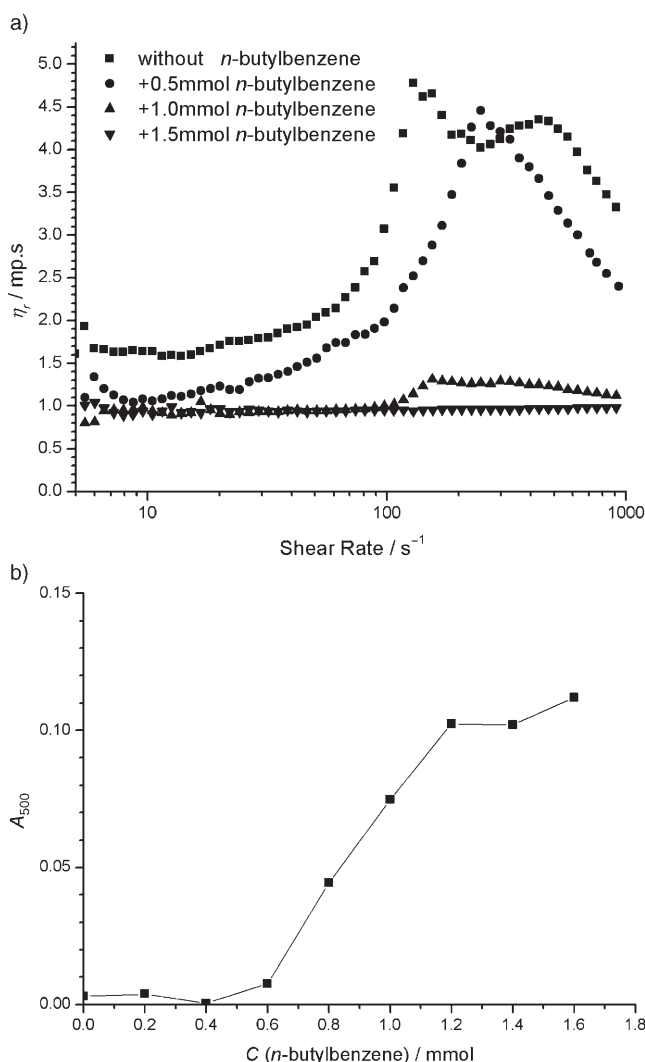

Figure 2. a) Steady-state rheological curves and b) variation of absorbance at 500 nm (the solid line is a guide to the eye) for the system DTEAB/SDS ($C_{total} = 10$ mmol, $X_{DTEAB} = 0.25$) with addition of *n*-butylbenzene.

(Figure 2b) indicates that larger aggregates are formed in the system.

The microstructural transformation induced by addition of *n*-butylbenzene to the system was also investigated by DLS and TEM. Before addition of *n*-butylbenzene, the plot of the apparent hydrodynamic radius distribution $f(R_{h,app})$ calculated by the CONTIN method (see Experimental Section), has a single peak with an average apparent hydrodynamics radius $\langle R_{h,app} \rangle$ of 8 nm (Figure 3a), which reflects a typical equivalent size of rodlike surfactant micelles. When 1.5 mmol of *n*-butylbenzene is introduced, the peak in the DLS plot shifts to the right, $\langle R_{h,app} \rangle$ increases from 8 to 83 nm (Figure 3a), and corresponding spherical vesicles with a diameter of 100–200 nm are observed by TEM (Figure 3b). In this case, the solution becomes a Newtonian fluid (Figure 2a) and the apparent viscosity η_a of the solution is 0.93 mPa s at 25 °C (Figure 2a), which is quite close to the viscosity of water (0.89 mPa s). The above results suggest that spherical vesicles probably become the dominant

aggregates when 1.5 mmol of *n*-butylbenzene is added. Thus, MVT by solubilization of *n*-butylbenzene is confirmed.

Investigation of other micellar DTEAB/SDS systems with $C_{total} = 10$ mmol showed MVT by solubilization of *n*-butylbenzene can take place within certain surfactant compositions in Figure 1, that is, from $X_{DTEAB} = 0.25$ to 0.33 and from $X_{DTEAB} = 0.86$ to 0.96. Hereafter, such regions are referred as the R_{eff} (effective MVT regions) of the additive.

MVT induced by addition of alkanes: When *n*-octane (C$_8$) is gradually added to the micellar DTEAB/SDS system with $C_{total} = 10$ mmol and $X_{DTEAB} = 0.25$, the solution remains transparent and homogeneous until small droplets of oil appear that suggest the saturation limit of *n*-octane solubilization. Combined with the results of rheology measurements (not shown), it can be concluded that the rodlike micelles are transformed into spherical swollen micelles by solubilization of C$_8$, like similar reports for other surfactant systems.[10] However, the situation is different for the DTEAB/SDS micellar system with $C_{total} = 10$ mmol and $X_{DTEAB} = 0.33$. A sharp increase in absorbance is observed as C$_8$ is added to the solution (Figure 4a). The DLS results also show that $\langle R_{h,app} \rangle$ increases remarkably from 25 to 95 nm on addition of 2 mmol of C$_8$ (Figure 4b). Correspondingly, spherical vesicles with a diameter of 100–250 nm are observed by TEM (Figure 5). These results demonstrate that MVT takes place on addition of C$_8$ to the system. Further investigations revealed that the R_{eff} of C$_8$ is from $X_{DTEAB} = 0.29$ to 0.33 and $X_{DTEAB} = 0.86$ to 0.90, which is narrower than that of *n*-butylbenzene.

n-Hexane (C$_6$) and *n*-dodecane (C$_{12}$) were also investigated. Both can induce MVT within certain ranges of surfactant composition. The R_{eff} values of the alkanes are listed in Table 1. The R_{eff} decreases with increasing hydrocarbon chain length.

Occurrence of a MVT and adjustment of the ratio of vesicles to micelles by addition of polar organic additives: Besides apolar hydrocarbons, the effects of two kinds of polar organic additives, namely, *n*-octanol and *n*-octylamine, on a MVT were also studied in the DTEAB/SDS system. A MVT by addition of *n*-octanol (C$_8$OH) can take place over the entire micellar region of Figure 1; this suggests that C$_8$OH is much more efficient in inducing a MVT than the above hydrocarbons. The ratio of vesicles to micelles can be conveniently controlled by addition of a small amount of C$_8$OH.

As mentioned above, the solution of DTEAB/SDS with $C_{total} = 10$ mmol and $X_{DTEAB} = 0.25$ is composed of rodlike micelles with an average $R_{h,app}$ of 8 nm by DLS (Figure 6a). After addition of 0.50 mmol of C$_8$OH, two distinct peaks can be clearly observed in the plot of $f(R_{h,app})$ versus $R_{h,app}$ (Figure 6b), which correspond to fast and the slow diffusion modes, respectively. The fast mode has a $\langle R_{h,app} \rangle$ of 5 nm, which is close to that of the original rodlike micelles, and it is reasonable to attribute this mode to diffusion of the micelles. The slow mode has an $\langle R_{h,app} \rangle$ of 220 nm. Correspond-
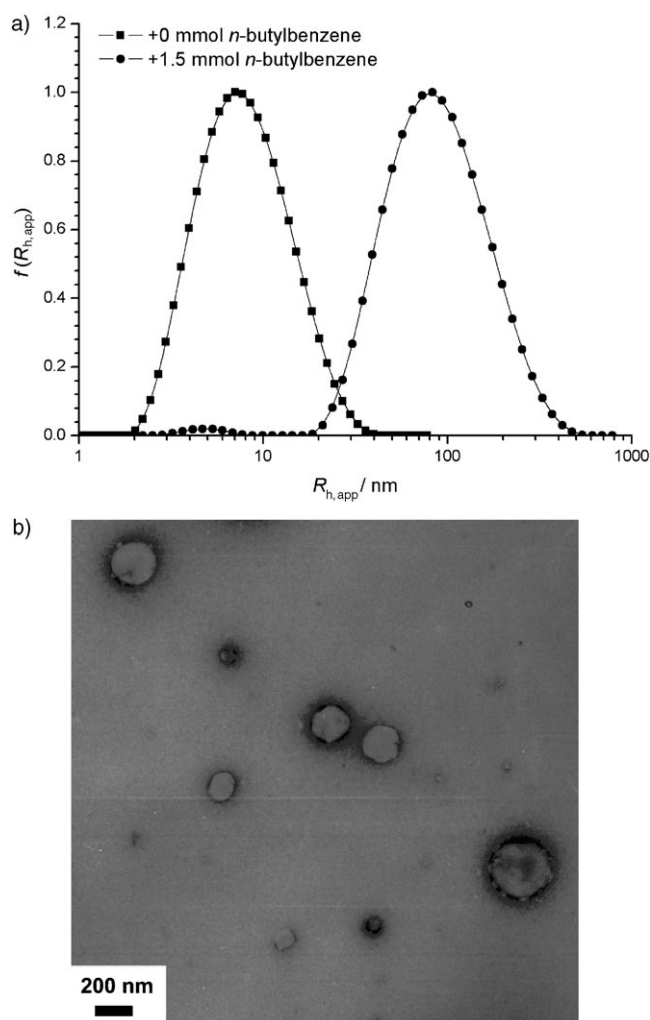
Figure 3. a) Plots of $f(R_{h,app})$ vs $R_{h,app}$ by DLS before and after addition of 1.5 mmol of *n*-butylbenzene and b) micrograph of vesicles by TEM after addition of 1.5 mmol of *n*-butylbenzene for the system DTEAB/SDS ($C_{total} = 10$ mmol, $X_{DTEAB} = 0.25$).
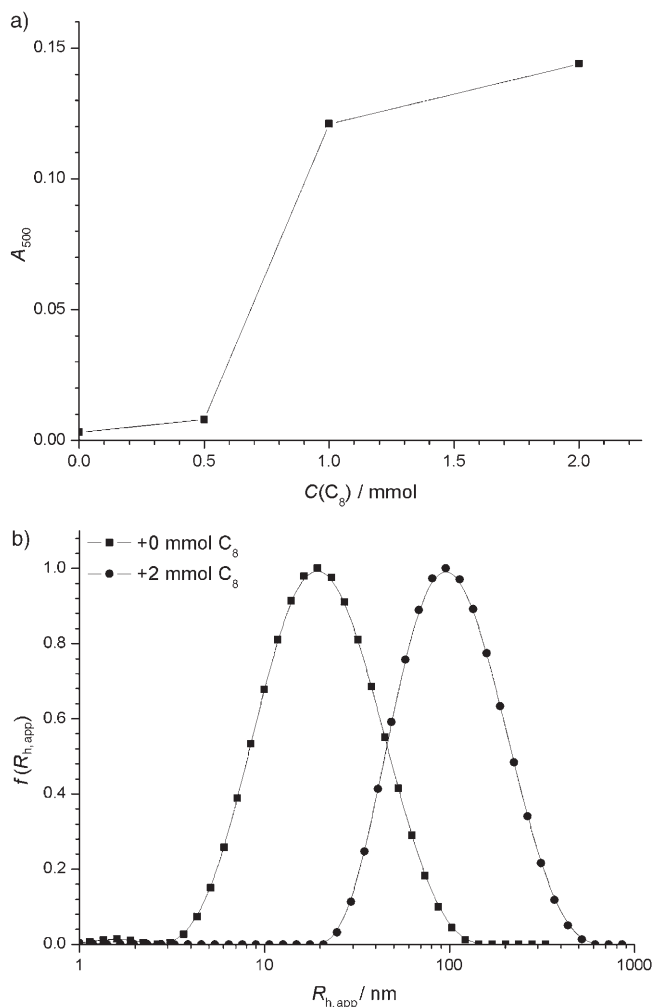
a)

b)

Figure 4. a) Variation of absorbance at 500 nm on addition of C_8 (the solid line is a guide to the eye) and b) plots of $f(R_{h,app})$ vs $R_{h,app}$ by DLS before and after addition of 2.0 mmol of C_8 for the system DTEAB/SDS ($C_{total}=10$ mmol, $X_{DTEAB}=0.33$).
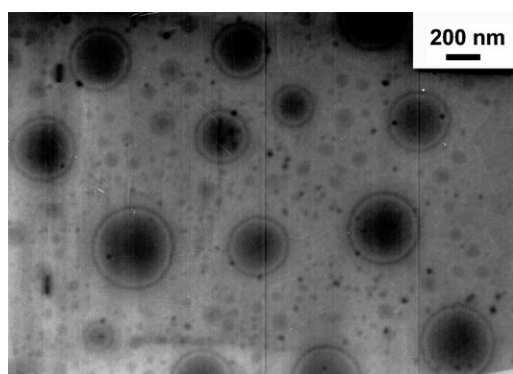

Figure 5. Micrograph of vesicles observed by TEM in the DTEAB/SDS system ($C_{total}=10$ mmol, $X_{DTEAB}=0.33$) on addition of 2 mmol of *n*-octane.

ingly, a few spherical vesicles with a diameter of 200–500 nm were observed by TEM (Figure 7a). Therefore, it can be de-

Table 1. R_{eff} for different hydrocarbons in the system DTEAB/SDS ($C_{total}=10$ mmol).

Alkanes	R_{eff}
C_6	0.26–0.33, 0.86–0.92
C_8	0.29–0.33, 0.86–0.90
C_{12}	0.32–0.33, 0.86–0.87

duced that the slow mode reflects the formation of vesicles in the solution. Therefore, the two peaks are designated as the "micelle peak" and the "vesicle peak" respectively. Further addition of C_8OH causes the micelle peak to shrink while the vesicle peak grows gradually (Figure 6c and d). Moreover, the contribution of the vesicle peak to the total scattering intensity of the sample I_v%, which is calculated from the weight of the vesicle peak area in the plot of $f(R_{h,app})$ versus $R_{h,app}$, also increases on addition of C_8OH (Figure 8a). These results indicate growing vesicle population and increasing ratio of vesicles to micelles. This tendency is further confirmed by TEM (Figure 7b and c). The variations of $\langle R_{h,app}\rangle$ for micelle and vesicle peaks as a function of C_8OH concentration are shown in Figure 8b. For the vesicles, $\langle R_{h,app}\rangle$ gradually decreases with increasing C_8OH concentration. When the amount of C_8OH reaches 1.5 mmol, the micelle peak almost disappears in the DLS plot (Figure 6e), and the vesicle peak has $\langle R_{h,app}\rangle$ of 79 nm. In this case, the rodlike micelles in the system are probably completely transformed into spherical vesicles.

The adjustment of the ratio of vesicles to micelles on C_8OH addition was also characterized by time-resolved fluorescence quenching (TRFQ) experiments. The time-dependent fluorescence intensity of a probe in the micelle in the presence of a quencher is thought to obey the Infelta–Tachiya equation [Eq. (1)],[11]

$$I(t) = I(0)\exp\{-A_2 t - A_3[1-\exp(-A_4 t)]\} \tag{1}$$

where A_2 and A_4 are independent of quencher concentration and A_3 is defined as Equation (2),

$$A_3 = N[Q]/C_m \tag{2}$$

where C_m is the concentration of surfactant in micellar form, [Q] the concentration of quencher, and N the average aggregation number of the micelles. In vesicles and other large aggregates, the time-dependent fluorescence intensity of a probe in the presence of a quencher is thought to obey the modified Stern–Volmer equation [Eq. (3)],[12]

$$I(t) = I(0)\exp\{-A_5 t - A_6 t^{1/2}\} \tag{3}$$

where A_5 and A_6 both depend on quencher concentration. When micelles and vesicles coexist in one system, the quenching kinetics will be governed by a linear combination of Equations (1) and (3). Unfortunately, the large number of parameters involved in such a combination makes quantitative analysis intractable. However, if the decay curves are
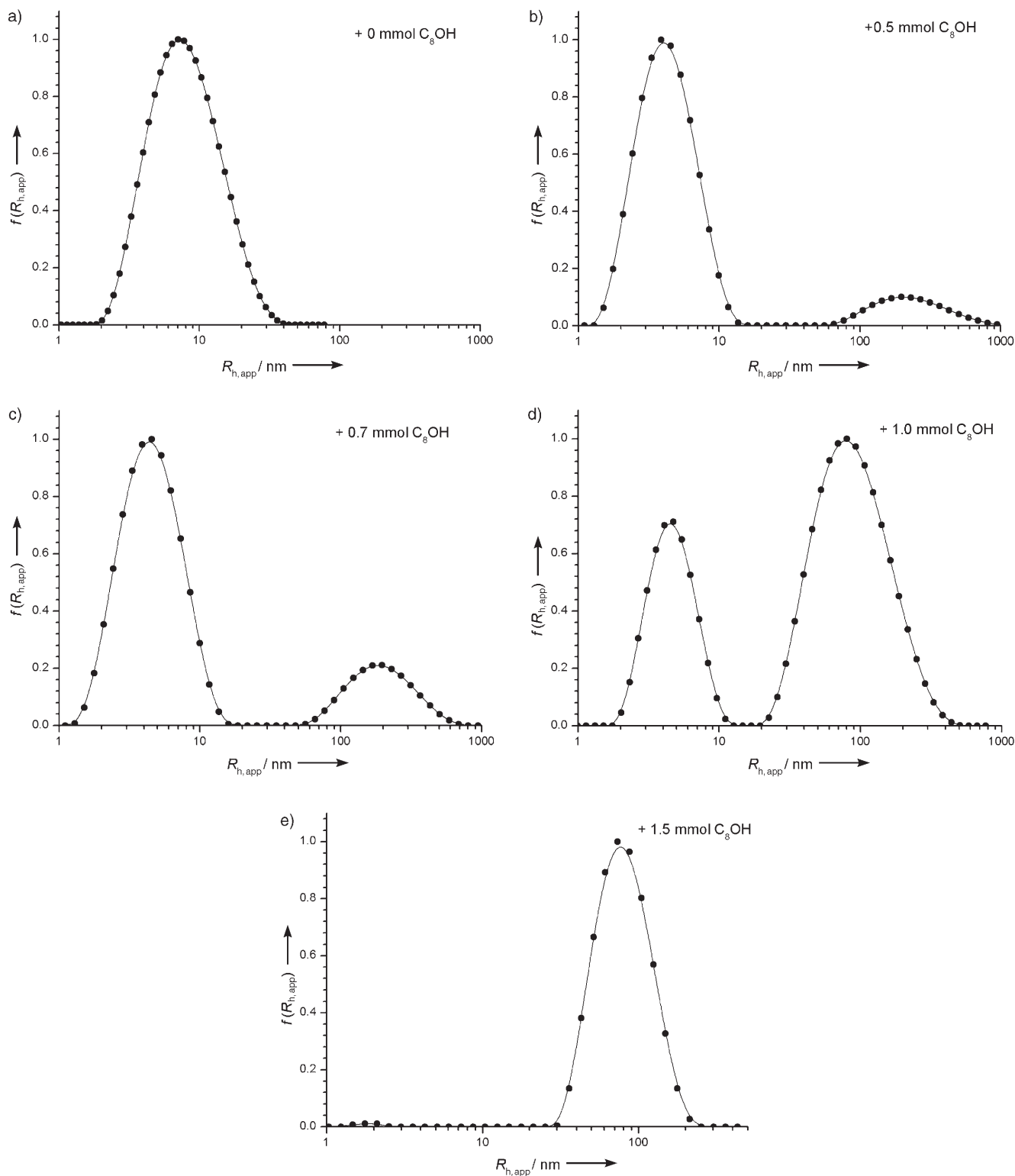
Figure 6. Distribution of apparent hydrodynamic radii $f(R_{h,app})$ of the system DTEAB/SDS ($C_{total} = 10$ mmol, $X_{DTEAB} = 0.25$) with different concentrations of C_8OH. a) 0, b) 0.50, c) 0.70, d) 1.0, and e) 1.5 mmol.

forced to fit the form of Equation (1), A_4 shows dependence on quencher concentration and the ratio of vesicles to micelles. By this method, TRFQ can be used to track the transition between micelles and vesicles. The TRFQ data for DTEAB/SDS mixtures with $C_{total} = 10$ mmol, $X_{DTEAB} = 0.25$, and different concentrations of C_8OH were measured. The variation of A_4 (obtained by fitting the data to [Eq. (1)]) as a function of η ($\eta = [Q]/C_{total}$) for these solutions is shown in
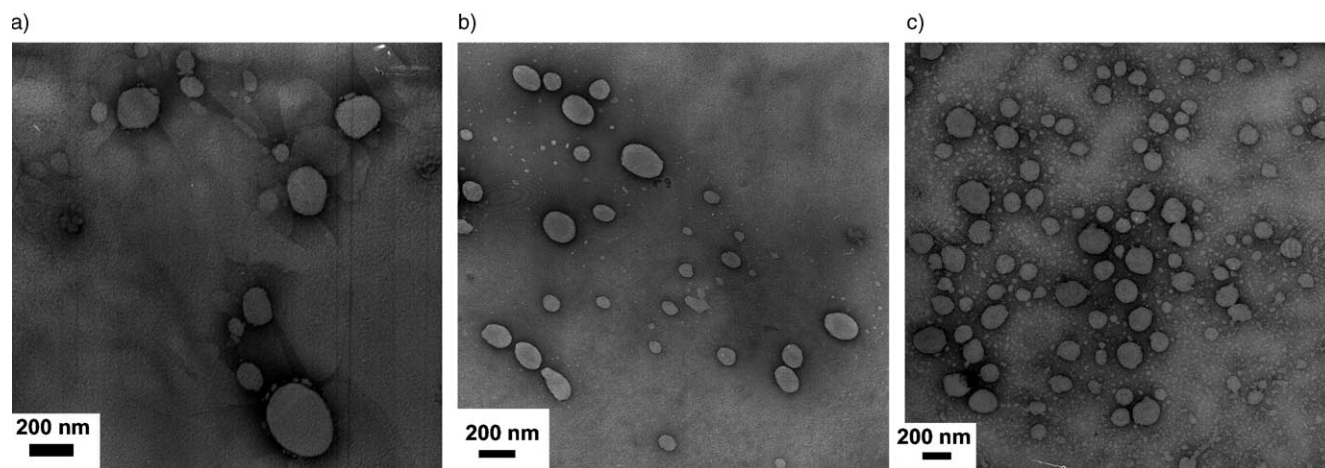
a)

b)

c)

Figure 7. Micrographs of vesicles (negative-staining technique) for the system DTEAB/SDS ($C_{total} = 10$ mmol, $X_{DTEAB} = 0.25$) on addition of a) 0.50, b) 1.0, and c) 1.5 mmol of C_8OH.
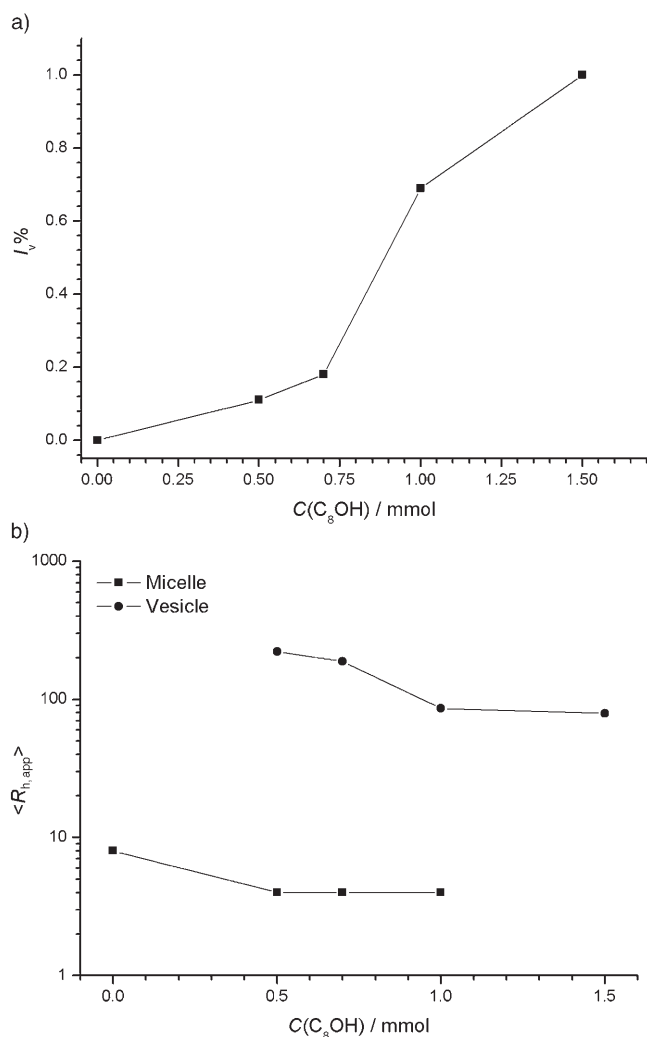
a)

b)

Figure 8. a) Variation of the contribution of the vesicle peak to the total scattering intensity of the solution $I_v\%$ as a function of the concentration of added C_8OH and b) $\langle R_{h,app} \rangle$ for the micelle and vesicle peaks as a function of $C(C_8OH)$ for the system DTEAB/SDS ($C_{total} = 10$ mmol, $X_{DTEAB} = 0.25$). The solid lines are visual aids.

Figure 9. Before C_8OH addition, A_4 is independent of η, that is, the solution is a pure micellar phase. The average aggregation number calculated from Equation (2) is 274 ± 15, which is also a typical value for rodlike micelles. On addition of 0.50 mmol of n-octanol, the slope of A_4 versus η begins to deviate from zero, and this suggests the formation of vesicles. Nevertheless, the dependence of A_4 on η is indistinctive, that is, the micelles are still the major component in the solution. With further addition of C_8OH, the slope of $A_4/A_{4,1}$ ($A_{4,1}$ is the value of A_4 when $\eta = 0.002$) versus η becomes increasingly positive (Figure 9), that is, the ratio of vesicles to micelles increases, as was proved by other studies.[7,13] Although the exact ratio of vesicles to micelles is difficult to obtain from the above measurements, it is confirmed that addition of C_8OH is an effective way of adjusting the ratio of vesicles to micelles in the DTEAB/SDS
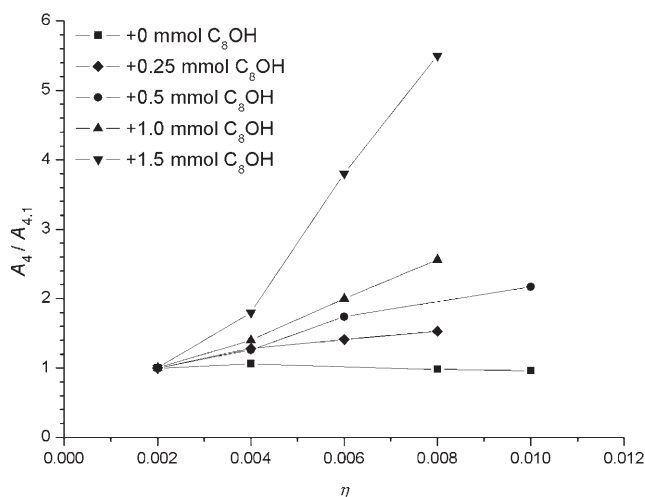

Figure 9. Normalized value of the parameter A_4 as a function of η ($\eta = [Q]/C_{total}$) with various concentrations of added C_8OH ($A_{4,1}$ is the value of A_4 when $\eta = 0.002$) for the system DTEAB/SDS ($C_{total} = 10$ mmol, $X_{DTEAB} = 0.25$). The solid lines are visual aids.

system, and thus vesicle/micelle solutions with variable ratio of vesicles to micelles can be easily obtained.

n-Octylamine (C_8NH_2) has the same hydrocarbon chain length as C_8OH but a different polar head group. Its R_{eff} also covers the entire micellar region of the DTEAB/SDS system with $C_{total} = 10$ mmol. For the DTEAB/SDS system ($C_{total} = 10$ mmol, $X_{DTEAB} = 0.25$), only 1.0 mmol of C_8NH_2 is required for complete MVT. In addition, similar to C_8OH, micelle/vesicle solutions can also be easily realized and actively controlled by addition of C_8NH_2.

MVT induced by organic additives in the DTEAB/SDSO$_3$ system: The solubilization behavior of the above organic additives was also studied in the *n*-dodecyltriethylammonium bromide/sodium *n*-dodecylsulfonate (DTEAB/SDSO$_3$) catanionic surfactant system with $C_{total} = 10$ mmol. None of the apolar hydrocarbons can induce a MVT in this system. However, the addition of C_8OH or C_8NH_2 can still efficiently

cause a MVT in the entire micellar region. Moreover, the ratio of vesicles to micelles can also be adjusted by addition of the polar additives. The solution of DTEAB/SDSO$_3$ with $C_{total} = 10$ mmol and $X_{DTEAB} = 0.25$ is selected as an instance. The micelles in this system have $\langle R_{h,app} \rangle = 2$ nm by DLS and an average aggregation number of 164 ± 10 by TRFQ. According to the DLS results (Figure 10) and TEM (Figure 11), the ratio of vesicles to micelles gradually increases on addition of C_8OH, and 2.5 mmol C_8OH is required for the complete MVT.

Discussion

Mechanism of hydrocarbon-induced MVT: As far as we know, this study is the first report that solubilization of a hydrocarbon (alkylbenzene or alkane) can induce a MVT in a surfactant system. It is known that the location, distribution,
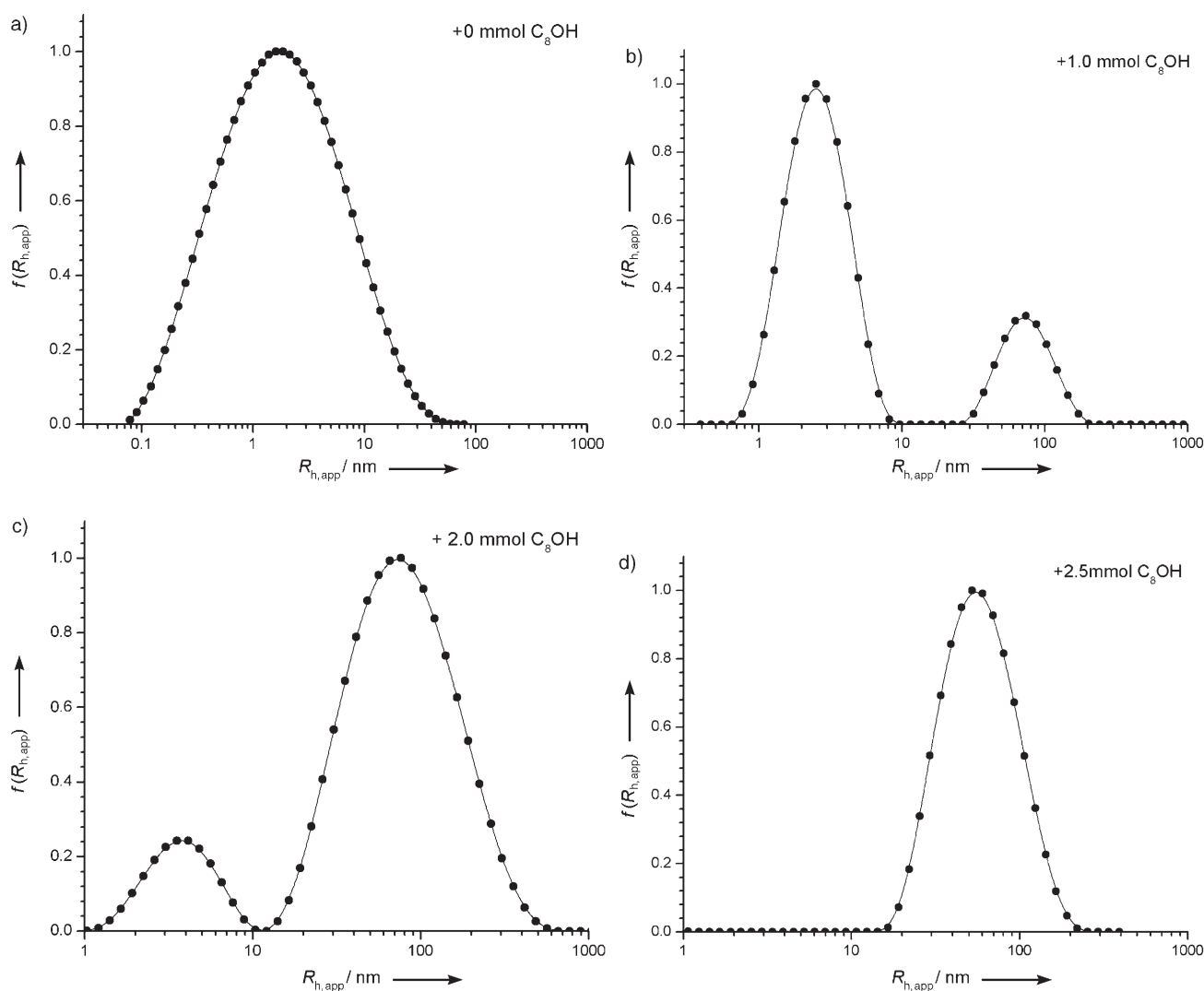

Figure 10. The apparent hydrodynamic radius distribution $f(R_{h,app})$ of the system DTEAB/SDSO$_3$ ($C_{total} = 10$ mmol, $X_{DTEAB} = 0.25$) with different concentrations of added C_8OH: a) 0, b) 1.0, c) 2.0, and d) 2.5 mmol.
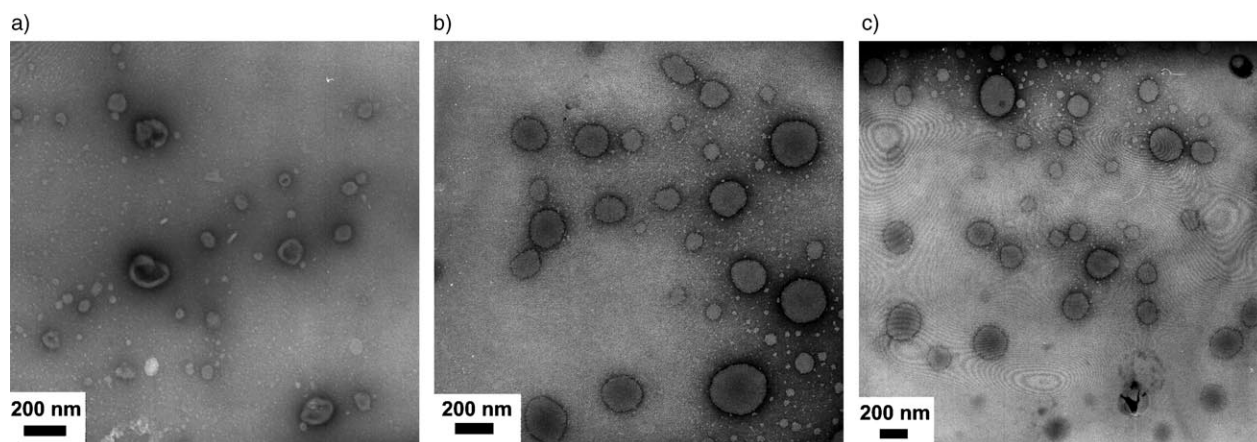
a)

b)

c)

Figure 11. Micrographs of vesicles (negative-staining technique) in the system DTEAB/SDSO$_3$ ($C_{total} = 10$ mmol, $X_{DTEAB} = 0.25$) on addition of a) 1.0, b) 2.0, and c) 2.5 mmol of C$_8$OH.

and orientation of the solubilized molecules can significantly influence the morphology of the aggregate.[14] Possible mechanisms for these phenomena are discussed below.

Previous studies have shown that the alkyl chain of alkylbenzene tends to dissolve in the palisade of the surfactant micelle with the benzene group located near the water/hydrocarbon interface,[15] and this increases the volume of the surfactant hydrocarbon tail. The well-known theory of the packing parameter p, proposed by Israelachvili et al.,[16] has been widely and successfully used to explain the transformations of organized assemblies in dilute surfactant solutions: $0 \leq p \leq 1/3$ for spherical micelles, $1/3 \leq p \leq 1/2$ for cylindrical micelles, and $1/2 \leq p \leq 1$ for bilayer structures (p is defined as $v/a_0 l_c$, where v is the surfactant tail volume, l_c is the tail length, and a_0 is the equilibrium area per molecule at the aggregate surface).[17] It is conceivable that, on solubilization of n-butylbenzene in the DTEAB/SDS system, the variation of a_0 and l_c will be insignificant. Therefore an increase in the aggregate parameter p can be expected, and formation of larger aggregates with lower curvature is more favored. In fact, spherical micelles were found to undergo transformation to rodlike micelles in some ionic surfactant systems on addition of alkylbenzenes, but no further transformation from rodlike micelles to vesicles was observed in these systems, probably because strong electrostatic repulsions between ionic head groups prevent further growth of the micelles. In catanionic surfactant systems, such as DTEAB/SDS mixtures, the electrostatic repulsions between identically charged molecules can be partly screened if not totally, depending on the mixing ratio of the two surfactants in the aggregate, by electrostatic attraction between the oppositely charged molecules, which makes the packing parameter p of the micelles larger than that of single SDS or DTEAB micelles. Therefore, at appropriate surfactant composition, the additional increase in p induced by the solubilization of n-butylbenzene may satisfy the requirements for vesicle formation and induce MVT in the system. Note that a qualitative rather than quantitative explanation based on the theory of the packing parameter is presented here, since it is

usually difficult to obtain the accurate value of a_0, which is quite dependent on aggregate composition and other environmental factors, such as counterion concentration. Although the value of a_0 is often substituted by the value of the area per molecule occupied at the air/water interface (obtained from adsorption data) when the surfactant concentration is near the critical micelle concentration (CMC), this approximation may cause considerable errors when the concentration of the investigated system is much higher than CMC (e.g., the total surfactant concentration in our studied systems is around 100 times CMC).

Based on our study, the R_{eff} of n-butylbenzene ($X_{DTEAB} = 0.25$–0.33 and 0.86–0.96) is close to the vesicular region on both the DTEAB-rich and SDS-rich sides (see Figure 1); this suggests that the micellar phases within R_{eff} have larger p parameters closer to those of vesicles than those outside R_{eff}. Therefore, it is possible that the capability of n-butylbenzene to increase the packing parameter is limited, so that for micellar phases outside R_{eff} the contribution of n-butylbenzene to increasing the p parameter cannot meet the requirement for the formation of vesicles, and no MVT is observed in these solutions.

As mentioned above, alkanes were usually considered to be solubilized in the micellar core of surfactant micelles and induce formation of swollen spherical micelles.[10] However, induction of a MVT by alkanes in the DTEAB/SDS system can not be satisfactorily explained if alkane molecules are merely solubilized in the micellar core. It was proposed that alkane molecules that have shorter hydrocarbon chains than the surfactant are not restricted to the interior of the micelle and can partially penetrate into the palisade layer of the micelle,[18] which will also promote an increase in the effective hydrocarbon tail volume v in the hydrophobic region. Hence, the solubilization of alkane, similar to the effect of n-alkylbenzene, may increase the packing parameter, and the MVT may then take place within certain ranges of surfactant composition in the catanionic surfactant system. In addition, the R_{eff} of the alkanes are generally narrower than that of n-butylbenzene, probably because the alkane mole-

cules are not completely solubilized in the micelle palisade and are still located close to the interior of the micelle, so that the ability of alkanes to increase the packing parameter is weaker than that of n-butylbenzene. Moreover, it was proposed that alkane molecules with longer chains have a stronger tendency to be solubilized in the hydrophobic core instead of the palisade of the surfactant micelle;[18a,19] hence, R_{eff} of alkanes becomes narrower with increasing hydrocarbon chain length (see Table 1). Thus, it is reasonable that the order of the ability of hydrocarbons to induce a MVT is n-alkylbenzene > n-hexane > n-octane > n-dodecane.

However, these hydrocarbons are not generally effective in inducing MVTs in various catanionic surfactant systems. None of the above hydrocarbons can induce a MVT in the micellar phase of DTEAB/SDSO$_3$ ($C_{total} = 10$ mmol), no matter how the surfactant ratio is varied, although the molecular structure of SDSO$_3$ is very similar to that of SDS except for the head group. The contrasting solubilization behaviors of the hydrocarbons may be correlated to the different molecular interactions between surfactant molecules in the two systems. Recently, we demonstrated[4b] that the DTEAB/SDSO$_3$ system exhibits weaker intermolecular interactions than the DTEAB/SDS system by comparison of the β parameters based on regular solution theory.[20] Therefore, it can be expected that the surfactant molecules in the DTEAB/SDSO$_3$ micelle are more loosely packed than those in the DTEAB/SDS micelle,[20b,c] and this may make the packing parameter and aggregation number smaller than those of the DTEAB/SDS micelle at similar surfactant composition. In fact, our TRFQ experiments have shown that at similar surfactant composition (e.g., $C_{total} = 10$ mmol and $X_{DTEAB} = 0.25$), the aggregation number of the DTEAB/SDSO$_3$ micelle is clearly smaller than that of the DTEAB/SDS micelle. Considering the limited contribution of the hydrocarbons to the increased packing parameter, it is reasonable to assume that the increase in the total aggregate packing parameter due to the presence of these hydrocarbons can not meet the requirements for vesicle formation in all micellar solutions of the DTEAB/SDSO$_3$ system with $C_{total} = 10$ mmol. Thus, it can be concluded that MVT cannot be induced by addition of hydrocarbons to catanionic systems in which the interactions between surfactant molecules are relatively weak.

High efficiency and activity of polar organic additives in inducing a MVT and adjusting the ratio of vesicles to micelles: The R_{eff} of both C$_8$OH and C$_8$NH$_2$ are much broader than those of the hydrocarbons in the DTEAB/SDS system ($C_{total} = 10$ mmol), and the polar additives can induce a MVT even in the DTEAB/SDSO$_3$ system ($C_{total} = 10$ mmol), whereas the hydrocarbons fail to do so under the same conditions, which demonstrates the superiority of polar organic additives over hydrocarbons in inducing MVTs. Polar organic additives, such as C$_8$OH, can preferentially penetrate into the palisade of surfactant micelles with their polar head group (OH group of C$_8$OH) towards the surface and thus act as a kind of co-surfactant with a rather small head

group. Besides the contribution of the hydrocarbon chain to increasing effective hydrocarbon tail volume v, the effect of the head group should also be considered. Previous work showed that solubilization of certain alcohols in lipid solution can significantly reduce the bending energy of the lipid multilayers and make the membranes more flexible.[21] Therefore, it is reasonable to think that the presence of the polar head group of the polar additive probably significantly alters the interactions between surfactant head groups in catanionioc surfactant systems and favors the formation of vesicles. Thus, the polar additives would have much higher efficiency and activity in inducing a MVT than the apolar hydrocarbons. It is also noteworthy that for the DEAB/SDS system ($C_{total} = 10$ mmol, $X_{DTEAB} = 0.25$), a lower concentration of C$_8$NH$_2$ (1.0 mmol) is required for a complete MVT compared with that of C$_8$OH (1.5 mmol). This difference may come from the partial protonation of C$_8$NH$_2$ to C$_8$NH$_3^+$ in water,[22] which can neutralize the excess negative charges in the aggregate and make an extra contribution to the increase in the packing parameter than the neutral C$_8$OH molecule. Hence C$_8$NH$_2$ will exhibit greater efficiency in inducing a MVT in micellar phases that are rich in anionic surfactant.

The ratio of vesicles to micelles can be adjusted by addition of relatively small amounts of polar organic compounds in both catanionic surfactant systems, and this may have potential applications in templated synthesis of materials. Recently, the synthesis of bimodal mesoporous materials has attracted special interest for their higher activities and better control of selectivity over monomodal porous materials.[23] Bimodal mesoporous materials with a well-defined pore size distribution on two different scales can be easily synthesized in one step by a dual-templating method[24] in which two different kinds of organized supermolecular assemblies simultaneously coexist in one phase (e.g., vesicle/micelle system) and separately control the bimodal pores. Although mixed vesicular/micellar phases exist in many catanionic surfactant systems and are quite promising for use as dual templates, the region of coexisting vesicle/micelle phases in the phase diagram is usually narrow.[1b,25] Therefore, it is difficult to actively control the ratio of vesicles to micelles by varying the surfactant ratio in catanionic surfactant systems, and so far few attempts[26] have been made to synthesize controlled bimodal mesoporous materials with this kind of dual templates. Our work may provide a novel and universal method to realize such goal. Micelle/vesicle solutions of catanionic surfactant systems generated by addition of polar additives could act as templates for synthesis of bimodal porous materials in which the two pore size distributions are separately controlled by the micelles and vesicles. Moreover, a series of dual-template systems with different ratios of vesicle to micelle can be easily obtained by gradual addition of polar additives, and thus the connection between the dual-template solutions and the structures, as well as the properties of synthesized materials, can also be systemically investigated, which may help to understand the complex template mechanism and find suitable templates

for other organized assemblies. Further study is ongoing in our laboratory.

Conclusion

It can be concluded that the induction of MVT in catanionic surfactant systems by addition of organic additives is closely related to the structure and polarity of the additive, the surfactant composition, and the interactions between the surfactant molecules. Addition of a nonpolar hydrocarbon with a certain chain length, such as *n*-butylbenzene or *n*-octane, can induce MVT at proper surfactant compositions in a catanionic surfactant system with relatively strong intermolecular interactions and high micelle aggregation number. Polar additives, such as *n*-octanol, are much more efficient in inducing MVT even in the system with weaker intermolecular interactions. Moreover, solubilization of the polar additive provides a series of two-template systems with variable ratios of vesicles to micelles for the synthesis of controlled bimodal mesoporous materials. This work may advance further understanding of the controlled transformation of organized assemblies in surfactant solutions and promote its applications in other fields.

Experimental Section

Materials: *n*-Dodecyltriethylammonium bromide (DTEAB) was prepared by reaction of 1-bromododecane and triethylamine and was recrystallized five times from ethanol/acetone. The purity of the surfactant was examined, and no minimum was found in the surface tension curve. Sodium *n*-dodecyl sulfate (SDS) and sodium *n*-dodecyl sulfonate (SDSO$_3$) were purchased from Acros Organics Co. and were used as received. The water used was redistilled from potassium permanganate. The other reagents were products of A.R. grade.

Sample preparation: Catanionic surfactant mixtures were prepared by mixing the single surfactant solutions directly in a test tube. Then the desired amount of organic additive was added to the tube by microsyringe. After stirring for several minutes, the sample was held thermostatically at 25°C for at least one week to reach equilibrium.

Dynamic light scattering (DLS): The hydrodynamic properties of the surfactant aggregates can be characterized by DLS. DLS measurements were performed with a spectrometer (ALV-5000/E/WIN Multiple Tau Digital Correlator) and a Spectra- Physics 2017 200 mW Ar laser ($\lambda = 514.5$ nm). The scattering angle was 90°. All solutions were filtered through a 0.4 μm filter into the cylindrical scattering cell before the experiment. Experimentally, the normalized intensity autocorrelation function $g^{(2)}(q,t)$ at delay time t and scattering vector q is measured first. q is defined as $q = (4\pi n_0/\lambda_0)\sin(\theta/2)$, where n_0 is the refractive index of the solvent and λ_0 is the wavelength of the incident light in vacuum. $g^{(2)}(q,t)$ can then be converted to the electric field autocorrelation function $g^{(1)}(q,t)$ by means of a Siegert relationship [Eq. (4)],[27]

$$g^{(2)}(q,t) = B\{1 + b|g^{(1)}(q,t)|^2\} \tag{4}$$

where B is the (infinite time) baseline and b is an optical constant. $g^{(1)}(q,t)$ can be written as the Laplace transformation of the distribution of relaxation rates $G(\Gamma)$ [Eq. (5)],

$$g^{(1)}(q,t) = \int_0^\infty G(\Gamma,q)\exp(-\Gamma t)d\Gamma \tag{5}$$

Laplace inversion of Equation (5) with the CONTIN program for peak-constrained analysis[28] supplied with the ALV-5000 digital time correlator yields the spectrum of decay rates for the various processes in the scattering samples as a series of amplitudes $G(\Gamma)$ along a grid of Γ values. Equation (5) can be modified as Equation (6),

$$g^{(1)}(q,t) = \int_0^\infty G(\Gamma,q)\exp(-\Gamma t)d\lg(\Gamma/q^2) \tag{6}$$

so that the plot is in an equal-area representation and the area under each $G(\Gamma)$ peak corresponds to the weight of the peak. The effective diffusion coefficient D_{eff} of the aggregates is defined by $D_{\text{eff}} = \Gamma/q^2$. Therefore, $G(\Gamma)$ obtained can be transformed into an effective coefficient distribution $G(D_{\text{eff}})$. Furthermore, $G(D_{\text{eff}})$ can be converted to the apparent hydrodynamic radius distribution $f(R_{\text{h,app}})$ by the well-known Stokes–Einstein equation $R_{\text{h,app}} = k_B T/(6\pi\eta D_{\text{eff}})$, where k_B is the Boltzmann constant, η the viscosity of the solvent, and T the absolute temperature of the solution. The Stokes–Einstein equation is only strictly valid for spherical particles. For asymmetrical particles, $R_{\text{h,app}}$ obtained from the Stokes–Einstein equation is the equivalent value corresponding to a sphere of the same diffusion coefficient.

Time-resolved fluorescence quenching (TRFQ): Pyrene was used as fluorescence probe, and dodecylpyridinium chloride (C$_{12}$PyCl) as quencher of the fluorescence probe. The desired amount of pyrene in ethanol and C$_{12}$PyCl in water were added to the surfactant solution directly, and then the solution was stirred vigorously for 48 h. The concentration of pyrene was kept low (1×10^{-6} M) to prevent excimer formation. The amount of ethanol in the surfactant solution was controlled to less than 1 vol%. All of the solutions were degassed by nitrogen for 15 min before the measurement to eliminate the influence of oxygen. Pyrene fluorescence decay curves were monitored by an Edinburgh FLS920 time-resolved fluorescence spectrophotometer (excitation at 337 nm and emission at 385 nm). The fluorescence decay of pyrene was fitted by using modified DECAN 1.0 software from the Key Laboratory of Photochemistry, CAS.

Absorbance measurements: Absorbance measurements were carried out with a Varian CARY 1E spectrophotometer at 500 nm.

Transmission electron microscopy (TEM): Samples for TEM were prepared by negative-staining technique with aqueous uranyl acetate solution. A JEM-100CX electron microscope was employed.

Rheology measurements: The rheological properties of samples were measured with a ThermoHaake RS300 rheometer. A double-gap cylindrical sensor system was used with an outside gap of 0.30 mm and an inside gap of 0.25 mm.

Acknowledgements

[1] a) E. W. Kaler, A. K. Murthy, B. E. Rodriguez, J. A. N. Zasadzinski, *Science* **1989**, *245*, 1371; b) E. W. Kaler, K. L. Herrington, A. K. Murthy, J. A. N. Zasadzinski, *J. Phys. Chem.* **1992**, *96*, 6698; c) K. L. Herrington, E. W. Kaler, D. D. Miller, J. A. Zasadzinski, S. Chiruvolu, *J. Phys. Chem.* **1993**, *97*, 13792; d) A. Caria, A. Khan, *Langmuir* **1996**, *12*, 6282; e) E. F. Marques, O. Regev, A. Khan, M. G. Miguel, B. Lindman, *J. Phys. Chem. B* **1998**, *102*, 6746; f) K. Horbaschek, H. Hoffmann, J. C. Hao, *J. Phys. Chem. B* **2000**, *104*, 2781; g) T. Kato, H. Takeuchi, T. Seimiya, *J. Phys. Chem.* **1992**, *96*, 6839; h) M. B. Sjöbom, H. Edlund, *Langmuir* **2002**, *18*, 8309; i) R. D. Koehler, S. R.

Raghavan, E. W. Kaler, *J. Phys. Chem. B* **2000**, *104*, 11035; j) M. Bergström, *Langmuir* **1996**, *12*, 2454.

[2] a) A. Helenius, K. Simons, *Biochim. Biophys. Acta* **1975**, *415*, 29; b) J. Fendler, *Membrane Mimetic Chemistry*, Wiley, New York, **1983**.

[3] a) P. Fromherz, *Chem. Phys. Lett.* **1983**, *94*, 259; b) D. D. Lasic, *Biochem. J.* **1988**, *256*, 1; c) M. M. Stecker, G. B. Benedek, *J. Phys. Chem.* **1984**, *88*, 6519.

[4] a) H. Q. Yin, Z. K. Zhou, J. B. Huang, R. Zheng, Y. Y. Zhang, *Angew. Chem.* **2003**, *115*, 2238; *Angew. Chem. Int. Ed.* **2003**, *42*, 2188; b) H. Q. Yin, J. B. Huang, Y. Y. Lin, Y. Y. Zhang, S. C. Qiu, J. P. Ye, *J. Phys. Chem. B* **2005**, *109*, 4104.

[5] L. L. Brasher, K. L. Herrington, E. W. Kaler, *Langmuir* **1996**, *12*, 4267.

[6] M. Mao, J. B. Huang, B. Y. Zhu, J. P. Ye, *J. Phys. Chem. B* **2002**, *106*, 219.

[7] a) M. Singh, C. Ford, V. Agarwal, G. Fritz, A. Bose, V. T. John, G. L. McPherson, *Langmuir* **2004**, *20*, 9931; b) H. Hoffmann, C. Thunig, D. Miller, *Colloids Surf. A* **2002**, *210*, 147; c) H. Hoffmann, K. Horbaschek, F. Witte, *J. Colloid Interface Sci.* **2001**, *235*, 33; d) R. Oda, L. Bourdieu, *J. Phys. Chem. B* **1997**, *101*, 5913; e) S. Chiruvolu, H. D. Warriner, E. Naranjo, S. H. J. Idziak, J. O. Rädler, R. J. Plano, J. A. Zasadzinski, C. R. Ssfinya, *Science* **1994**, *266*, 1222; f) H. Hoffmann, G. Ebert, *Angew. Chem.* **1988**, *100*, 933; *Angew. Chem. Int. Ed. Engl.* **1988**, *27*, 902.

[8] a) C. Z. Wang, S. H. Tang, J. B. Huang, X. R. Zhang, H. L. Fu, *Colloid Polym. Sci.* **2002**, *280*, 770; b) X. R. Zhang, J. B. Huang, M. Mao, S. H. Tang, B. Y. Zhu, *Colloid Polym. Sci.* **2001**, *279*, 1245.

[9] a) R. Bruinsma, W. Gelbart, A. B. Shaul, *J. Chem. Phys.* **1992**, *96*, 7710; b) S. Q. Wang, *J. Phys. Chem.* **1990**, *94*, 8381; c) S. Hofmann, H. Hoffmann, *J. Phys. Chem. B* **1998**, *102*, 5614; d) Cl. Oelschlaeger, G. Waton, S. J. Candau, M. E. Cates, *Langmuir* **2002**, *18*, 7265; e) R. Oda, P. Panizza, M. Schmutz, F. Lequeux, *Langmuir* **1997**, *13*, 6407.

[10] a) R. Nagarajan, *Curr. Opin. Colloid Interface Sci.* **1996**, *1*, 391; b) O. Bayer, H. Hoffmann, W. Ulbricht in *Surfactants in Solution, Vol. 4*, Plenum, New York, **1987**, Part I, p. 343.

[11] a) M. Almgren, J. E. J. Löfroth, *J. Colloid Interface Sci.* **1981**, *81*, 486; b) M. Tachiya, *Chem. Phys. Lett.* **1975**, *33*, 289; c) M. Almgren, *Adv. Colloid Interface Sci.* **1992**, *41*, 9; d) M. H. Gehlen, F. C. De Schryver, *Chem. Rev.* **1993**, *93*, 199.

[12] a) F. Caruso, F. Grieser, A. Murphy, P. Thistlethwaite, R. Urquhart, M. Almgren, E. Wistus, *J. Am. Chem. Soc.* **1991**, *113*, 4838; b) B. Medhage, M. Almgren, *J. Fluoresc.* **1992**, *2*, 7.

[13] a) D. D. Miller, L. J. Magid, F. D. Evans, *J. Phys. Chem.* **1990**, *94*, 5921; b) O. Sonderman, K. L. Herrington, E. W. Kaler, D. D. Miller, *Langmuir* **1997**, *13*, 5531.

[14] a) H. Hoffmann, W. Ulbricht, *J. Colloid Interface Sci.* **1989**, *129*, 388; b) P. Mukerjee, J. R. Cardinal, *J. Phys. Chem.* **1978**, *82*, 1620; c) R. Nagarajan, M. A. Chaiko, E. Ruchenstein, *J. Phys. Chem.* **1984**, *88*, 2916.

[15] a) S. Kumar, A. Z. Naqvi, Kabir-ud-Din, *Langmuir* **2001**, *17*, 4787; b) N. Hedin, R. Sitnikov, I. Furó, U. Henriksson, O. Regev, *J. Phys. Chem. B* **1999**, *103*, 9631; c) P. M. Lindemuth, G. L. Bertrand, *J. Phys. Chem.* **1993**, *97*, 7769; d) M. B. Smith, A. E. Alexander, *Proceedings of the 2nd International Congress of Surface Activity, Vol. 1*, Butterworth, London, **1957**, p. 311.

[16] a) J. N. Israelachvili, D. J. Mitchell, B. W. Ninham, *J. Chem. Soc. Faraday Trans. 2* **1976**, *72*, 1525; b) J. N. Israelachvili, D. J. Mitchell, B. W. Ninham, *Biochim. Biophys. Acta* **1977**, *470*, 185; c) J. N. Israelachvili, S. Marcelja, R. G. Q. Horn, *Q. Rev. Biophys.* **1980**, *13*, 121.

[17] a) R. Nagarajan in *Structure-Performance Relationships in Surfactants* (Eds.: K. Esumi, M. Ueno), Marcel Dekker, New York, **1997**, Chap. 1, pp. 1–89; b) K. A. Dill, P. J. Flory, *Proc. Natl. Acad. Sci. USA* **1980**, *77*, 3115; c) A. Ben-Shaul, I. Szleifer, W. M. Gelbart, *Proc. Natl. Acad. Sci. USA* **1984**, *81*, 4601; d) S. Puvvada, D. Blankschtein, *J. Phys. Chem.* **1992**, *96*, 5567.

[18] a) B. Bumgdad, J. Eastoe, R. K. Heenan, J. R. Lu, D. C. Steytler, S. Egelhaad, *J. Chem. Soc. Faraday Trans.* **1998**, *94*, 2143; b) L. E. Scriven, *J. Chem. Phys.* **1983**, *79*, 11; c) F. Lichterfeld, T. Schmeling, R. Strey, *J. Phys. Chem.* **1986**, *90*, 5762.

[19] J. Penfold, E. Staples, I. Tucker, *J. Phys. Chem. B* **2002**, *106*, 8891.

[20] a) B. Jonsson, B. Lindman, K. Holmberg, B. Kronberg, *Surfactants and Polymers in Aqueous Solution*, Wiley, New York, **1998**; b) *Mixed Surfactant Systems* (Eds.: P. M. Holland, D. N. Rubingh) ACS Symposium Series 501, American Chemical Society, Washington, DC, **1992**, Chaps. 1 and 2; c) S. R. Raghavan, G. Fritz, E. W. Kaler, *Langmuir* **2002**, *18*, 3797.

[21] C. R. Safinya, E. B. Sirota, D. Roux, G. S. Smith, *Phys. Rev. Lett.* **1989**, *62*, 1134.

[22] Kabir-ud-Din, S. Kumar, Kirti, P. S. Goyal, *Langmuir* **1996**, *12*, 1490.

[23] a) M. Almgren, J. E. Löfroth, *J. Colloid Interface Sci.* **1981**, *81*, 486; b) M. Tachiya, *Chem. Phys. Lett.* **1975**, *33*, 289; c) M. H. Gehlen, F. C. De Schryver, *Chem. Rev.* **1993**, *93*, 199; d) F. Caruso, F. Grieser, A. Murphy, P. Thistlethwaite, R. Urquhart, M. Almgren, E. Wistus, *J. Am. Chem. Soc.* **1991**, *113*, 4838.

[24] a) D. M. Antonelli, *Microporous Mesoporous Mater.* **1999**, *33*, 209; b) J. L. Blin, A. Léonard, Z. Y. Yuan, L. Gigot, A. Vantomme, A. K. Cheetham, B. L. Su, *Angew. Chem.* **2003**, *115*, 2978; *Angew. Chem. Int. Ed.* **2003**, *42*, 2872.

[25] a) M. T. Yatcilla, K. L. Herrington, L. L. Brasher, E. W. Kaler, S. Chiruvolu, J. A. Zasadzinski, *J. Phys. Chem.* **1996**, *100*, 5874; b) A. J. O'Connor, T. A. Hatton, A. Bose, *Langmuir* **1997**, *13*, 6931; c) M. Bergström, J. S. Pedersen, *Langmuir* **1999**, *15*, 2250.

[26] a) J. G. C. Shen, *J. Phys. Chem. B* **2004**, *108*, 44; b) A. Lind, B. Spliethoff, M. Lindén, *Chem. Mater.* **2003**, *15*, 813.

[27] a) B. J. Berne, R. Pecora, *Dynamic Light Scattering*, Wiley, New York, **1976**; b) B. Chu, *Laser Light Scattering*, 2nd ed., Academic Press, New York, **1991**.

[28] a) S. W. Provencher, J. Hendrix, L. D. Maeyer, *J. Chem. Phys.* **1978**, *69*, 4273; b) S. W. Provencher, *Makromol. Chem.* **1979**, *180*, 201; c) S. W. Provencher, *Comput. Phys. Commun.* **1982**, *27*, 213.